Sugar-Based Gemini Surfactants with pH-Dependent Aggregation Behavior: Vesicle-to-Micelle Transition, Critical Micelle Concentration, and Vesicle Surface Charge Reversal

ARTICLE *in* LANGMUIR · MAY 2003

Impact Factor: 4.46 · DOI: 10.1021/la0343270

4 AUTHORS, INCLUDING:

Markus Johnsson
Camurus AB, Lund, Sweden
31 PUBLICATIONS **1,545** CITATIONS
SEE PROFILE

Marc C A Stuart
University of Groningen
137 PUBLICATIONS **3,917** CITATIONS
SEE PROFILE

Sugar-Based Gemini Surfactants with pH-Dependent Aggregation Behavior: Vesicle-to-Micelle Transition, Critical Micelle Concentration, and Vesicle Surface Charge Reversal

Markus Johnsson,*,† Anno Wagenaar, Marc C. A. Stuart, and Jan B. F. N. Engberts*

Stratingh Institute, Physical Organic Chemistry Unit, University of Groningen, Nijenborgh 4, 9747 AG Groningen, The Netherlands

Received February 25, 2003. In Final Form: March 25, 2003

In a recent report, we presented data on the rich and unusual pH-dependent aggregation behavior of a sugar-based (reduced glucose) gemini surfactant (Johnsson et al. *J. Am. Chem. Soc.* **2003**, *125*, 757). In the present study, we extend the previous investigation by introducing a different sugar headgroup (reduced mannose), by varying the spacer between the two main surfactant parts, and by introducing, in one of the surfactants, an amide linkage (instead of an amine linkage) between the headgroup and the unsaturated (C18:1) hydrocarbon tails. The aggregation behavior of these four gemini surfactants has been studied and compared by means of light scattering, cryo-transmission electron microscopy, electrophoretic mobility, and fluorescence measurements. We find that all four surfactants form vesicles near neutral or high pH. However, the vesicles made from the amine-containing geminis are transformed into cylindrical or wormlike micelles at lower pH values (pH < ∼5.5). The micellization is driven mainly by an increased electrostatic repulsion, caused by the protonation of the tertiary amino groups, and we find that the nature of the sugar or spacer has little influence on this process. At low pH (pH 2), solely small globular micelles are found, and the critical micelle concentration at this pH is about 0.005−0.010 mM for the different amine-containing surfactants. As was expected, the gemini surfactant with the amide instead of the amine functional groups in the headgroup does not undergo the vesicle-to-micelle transition but displays only vesicle formation within the investigated pH range. The electrophoretic mobility measurements on the vesicular samples formed from the amine-containing geminis show that the vesicles are cationic below pH ∼7−7.5; however, the vesicles acquire a substantial *negative* charge at a higher pH. The most probable explanation for this charge reversal is a strong adsorption (or binding) of hydroxide ions onto the vesicle surface. In accordance with this hypothesis, we find that the vesicles made from the amide-containing gemini are anionic (no protonation) even at a low pH (pH <5). Using a simple Poisson−Boltzmann model, we are able to describe the obtained ζ-potential profiles reasonably well and derive a hydroxide-ion binding constant (K_{OH}) for the respective systems. We find that the nature of the sugar does have a small influence on K_{OH}. The colloidal stability of all four types of the gemini vesicles seems to be well-described by the classical Derjaguin−Landau−Verwey−Overbeek theory, and the vesicles aggregate/flocculate rapidly in the limit of low surface potential. However, the flocculated vesicles can be easily redispersed by, for example, raising the pH of the solution, and this flocculation/redispersal process is completely reversible.

Introduction

A rather large number of studies on the aggregation behavior of gemini surfactants, or dimeric surfactants, have been published in the recent years.[1−4] The reason for the intense research is largely that these surfactants, in general, display properties that are quite different from those of conventional surfactants. Moreover, a lower critical micelle concentration (cmc) and a greater ability to lower the surface tension compared to those of conventional surfactants offers obvious practical advantages.[1,2] It appears likely that gemini surfactants will acquire some important industrial and biomedical applications. In this respect, it should be emphasized that the design of new gemini surfactants, of course, requires the interplay between surface and colloid scientists and synthetic organic chemists. This is especially obvious when more intricate structural variations are required.

In a recent study, we reported on the extraordinary aggregation behavior of a sugar-based gemini surfactant (**GS1**) in a dilute aqueous solution.[5] We showed that vesicles formed from **GS1** (Figure 1) are transformed into cylindrical or wormlike micelles at an acidic pH. The effect of the solution pH on the aggregation state stems from the presence of two tertiary nitrogens in the headgroup of **GS1**. The protonation of these nitrogens results in increased electrostatic repulsions between the headgroups and, thus, in a pH-dependent spontaneous curvature. Moreover, in the vesicular pH region, we found an unexpected vesicle surface charge reversal; that is, the vesicles were cationic below pH 7.1 but became anionic at a higher pH. The probable cause for this behavior is a strong binding of OH^- ions to the vesicle surface, and we used a Poisson−Boltzmann (PB) model to quantify a hydroxide ion binding constant.[5]

Herein, we have investigated the effect of changing the spacer or identity of the sugar headgroup (**GS2** and **GS3**, Figure 1 and Table 1). Furthermore, we have synthesized and characterized a gemini surfactant **GS4** that has no titratable functionalities (within the investigated pH interval) in the headgroup. The overall results for **GS2**

* Corresponding authors. E-mail: m.johnsson@chem.rug.nl (M.J.); j.b.f.n.engberts@chem.rug.nl (J.B.F.N.E.).

† Present address: Department of Physical Chemistry, Uppsala University, P.O. Box 579, SE-751 23 Uppsala, Sweden.

(1) Zana, R. *Adv. Colloid Interface Sci.* **2002**, *97*, 205.

(2) Menger, F. M.; Keiper, J. S. *Angew. Chem., Int. Ed.* **2000**, *39*, 1906.

(3) Bhattacharya, S.; Haldar, J. *Colloids Surf., A* **2002**, *205*, 119.

(4) Zana, R. *J. Colloid Interface Sci.* **2002**, *248*, 203.

(5) Johnsson, M.; Wagenaar, A.; Engberts, J. B. F. N. *J. Am. Chem. Soc.* **2003**, *125*, 757.

10.1021/la0343270 CCC: $25.00
Published on Web 05/01/2003

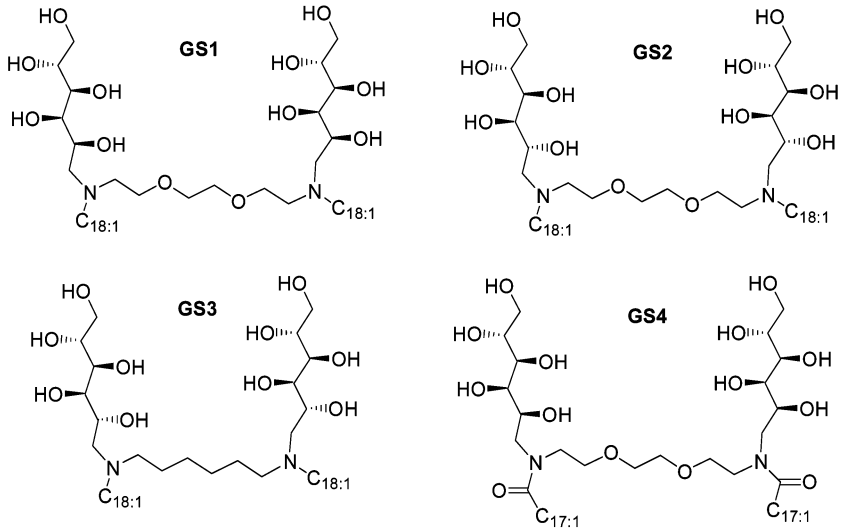

Figure 1. Structures of the four gemini surfactants investigated in this study (see also Table 1).

Table 1. Characteristics of the Gemini Surfactants

compound	hydrocarbon tail	spacer	headgroup (reduced sugar)
GS1	oleyl, C18:1 Δ^9, 75% cis	$-(EO)_2-(CH_2)_2-$	glucose
GS2	oleyl, C18:1 Δ^9, 75% cis	$-(EO)_2-(CH_2)_2-$	mannose
GS3	oleyl, C18:1 Δ^9, 75% cis	$-(CH_2)_6-$	mannose
GS4 (amide)	oleoyl, C18:1 Δ^9, 100% cis	$-(EO)_2-(CH_2)_2-$	glucose

and **GS3** are similar to those reported for **GS1**.[5] The vesicle-to-spherical-micelle transition proceeds via the formation of cylindrical micelles, as was detected by light scattering and cryo-transmission electron microscopy (cryo-TEM). This feature is quite uncommon for a single surfactant, at constant concentration, in dilute aqueous solution. However, there exist a few systems that display a similar "protonation-driven" behavior.[6−8] The vesicle surface charge reversal, observed for **GS1**,[5] is found also for **GS2** and **GS3**. As with the **GS1** vesicles, it appears to be due to a strong OH^- binding. This result is in line with recent studies on the charging of a variety of "neutral" surfaces in water; however, there is no conclusive evidence for the mechanism of OH^- binding.[9−14] We find in the present study that the nature of the sugar headgroup or spacer has only marginal effects on the binding. Furthermore, the **GS4** vesicles display a similar OH^- binding, thus, ruling out amines in the headgroup as responsible for the observed effect.

The colloidal stability of all four types of vesicles (**GS1**−**GS4**) is well-described by the classical Derjaguin−Landau−Verwey−Overbeek (DLVO) theory of colloidal stability.[15] In fact, even for the net neutral **GS4** surfactant, a rapid vesicle flocculation is observed at acidic pH where the OH^- concentration is low; thus, the *negative* surface charge density is low. The same behavior has been observed for "neutral" glycolipid vesicles,[9,10] and it seems that electrostatics have a great influence on the colloidal stability of vesicles prepared from a number of neutral, biologically relevant lipids.[9,10,16,17]

Experimental Section

Materials. Pyrene was obtained from Sigma-Aldrich, and dioleoyl phosphatidylcholine (DOPC) was purchased from Avanti Polar Lipids. All other salts and reagents were of analytical grade and were used as received.

Synthesis. The syntheses of compounds **GS1**−**GS4** are described in the Supporting Information.

Sample Preparation. Vesicle dispersions of **GS1**−**GS4** and DOPC (5 mM) were prepared at pH 6.7 by a brief tip sonication (<5 min at 35 °C) of the compounds in bidistilled water containing 5 mM each of the buffer substances Hepes, Mes, and NaAc (unless otherwise indicated). The resulting bluish (weakly turbid) dispersions were freeze-thawed [N_2(l) ↔ water bath, 50 °C] 3−5 times followed by extrusion (15 times) through 200-nm-pore-sized polycarbonate filters.

The samples for light scattering and electrophoretic mobility measurements were prepared by diluting the vesicle stock solution to 0.5 mM (unless otherwise indicated) and titrating the samples to the required pH [HCl(aq) or NaOH(aq)]. The pH was measured using a semimicro ROSS combination pH electrode from Thermo Orion, U.K.

Light Scattering. The static and dynamic light scattering (SLS and DLS) measurements were carried out at 25 °C on a Zetasizer 5000 instrument (Malvern Instruments, Ltd., U.K.) at a wavelength (λ_0) of 633 nm. The SLS and DLS measurements on the micellar samples were performed at a surfactant concentration of 5 mM because of the weak scattering of these samples. The micellar samples were centrifuged for 15 min at 2000 rpm before the measurements to remove any interfering dust particles from the scattering volume. The angular dependence of the scattered light intensity was measured between $50 \leq \theta \leq 130°$, and 25 angles were measured. The intensity data were normalized using toluene as a reference standard and

(6) Edwards, K.; Silvander, M.; Karlsson, G. *Langmuir* **1995**, *11*, 2429.
(7) Kawasaki, H.; Souda, M.; Tanaka, S.; Nemoto, N.; Karlsson, G.; Almgren, M.; Maeda, H. *J. Phys. Chem. B* **2002**, *106*, 1524.
(8) Morigaki, K.; Walde, P.; Misran, M.; Robinson, B. H. *Colloids Surf., A* **2003**, *213*, 37.
(9) Baba, T.; Zheng, L.-Q.; Minamikawa, H.; Hato, M. *J. Colloid Interface Sci.* **2000**, *223*, 235.
(10) Zheng, L.-Q.; Shui, L.-L.; Shen, Q.; Li, G.-Z.; Baba, T.; Minamikawa, H.; Hato, M. *Colloids Surf., A* **2002**, *207*, 215.
(11) Marinova, K. G.; Alargova, R. G.; Denkov, N. D.; Velev, O. D.; Petsev, D. N.; Ivanov, I. B.; Borwankar, R. P. *Langmuir* **1996**, *12*, 2045.
(12) Bergeron, V.; Waltermo, Å.; Claesson, P. M. *Langmuir* **1996**, *12*, 1336.
(13) Karraker, K. A.; Radke, C. J. *Adv. Colloid Interface Sci.* **2002**, *96*, 231.
(14) Stubenrauch, C.; Schlarmann, J.; Strey, R. *Phys. Chem. Chem. Phys.* **2002**, *4*, 4504.
(15) Evans, D. F.; Wennerström, H. *The Colloidal Domain*: *Where Physics, Chemistry, Biology and Technology Meet*; VCH Publishers Inc.: New York, 1994.
(16) Webb, M. S.; Tilcock, C. P. S.; Green, B. R. *Biochim. Biophys. Acta* **1988**, *938*, 323.
(17) Webb, M. S.; Green, B. R. *Biochim. Biophys. Acta* **1990**, *1030*, 231.

analyzed using the Guinier approximation[18]

$$I(\theta) \propto \exp(-q^2 R_g^2/3), \quad qR_g \ll 1 \tag{1}$$

where q is the scattering vector [$q = (4\pi n_s/\lambda_0)\sin(\theta/2)$, where n_s is the refractive index of the solvent] and $R_g = \langle R_g^2\rangle_z^{1/2}$ in which $\langle R_g^2\rangle_z$ is the z-average mean square radius of gyration of the aggregates.

The intensity autocorrelation functions obtained from DLS were analyzed using CONTIN[19] in all cases, and the measurements were performed at five different angles (50−130°). The obtained relaxation rate, Γ, is related to the translational diffusion coefficient, D_c, via

$$D_c = \Gamma/q^2 \tag{2}$$

The *apparent* hydrodynamic radius, R_h, was obtained from D_c using the Stokes−Einstein relation

$$D_c = k_B T/6\pi\eta R_h \tag{3}$$

where $k_B T$ is the Boltzmann temperature and η is the solvent viscosity. Note that eq 3 is strictly valid only at infinite dilution; that is, we are neglecting any concentration dependence of D_c.

Electrophoretic Mobility (ζ-Potential). The electrophoretic mobility (u) measurements were carried out using the Zetasizer instrument on vesicular samples, prepared as described above, in either 15 mM buffer or 15 mM NaCl containing 0.5 mM surfactant. The samples obtained after titration to the required pH were equilibrated for at least 1 h before starting the measurements. The results obtained after longer equilibration times (>12 h) were within the experimental error identical to that for the results obtained after 1 h. Before each series of measurements, the Zetasizer instrument was calibrated using a ζ-potential standard solution (latex standards) supplied by Malvern Instruments, U.K. The electric field strength in the cell was 19 V/cm, and the temperature was kept at 25 °C.

There are several theories relating the electrophoretic mobility to the particle ζ-potential. The most commonly used theory in the domain where the well-known Hückel and Smoluchowski limits do not apply is the Henry theory.[20] The Henry equation accounts for the retardation effects; however, it does not take into account relaxation effects that become important at high potential.[21] In this paper, we have calculated the ζ-potential using either the Henry equation (eq 4) or the theory developed by Oshima et al.[22] The latter theory accounts for relaxation effects and yields results that are consistent with the numerical calculations of O'Brien and White.[23] The Henry equation reads

$$\zeta = 3\eta u/2\epsilon_r\epsilon_0 f(\kappa, R) \tag{4}$$

where η, $\epsilon_r\epsilon_0$, κ, and R are the viscosity of the aqueous medium, permittivity of water, inverse of the Debye length, and vesicle radius, respectively. The function $f(\kappa, R)$ was set equal to 1.39 ($\kappa = 0.403\ \text{nm}^{-1}$, $R = 80$ nm). For clarity reasons, we have chosen to present the ζ-potential data calculated using the more elaborate Oshima−Healy−White theory[22] in the figures, but it is important to note that as long as the potential is less than ∼|50 mV|, the difference between the two theories is small (<10%).

cmc Measurements. The cmc of **GS1**−**GS3** at pH 2 was determined using pyrene fluorescence at 25 °C.[24] The characteristic intensity ratio, the I_1/I_3 ratio, was determined as a function of the surfactant concentration using a SLM SPF-500C spectrofluorometer ($\lambda_{exc} = 335$ nm, $\lambda_{em} = 368$−390 nm). The cmc was identified as the midpoint of the transition from high to low values of the I_1/I_3 ratio. The cmc measurements were performed in a medium containing 10 mM HCl and 5 mM NaCl (pH 2). Concentrated stock solutions of gemini **GS1**−**GS3** (HCl salts) were prepared in volumetric flasks by adding the solvent to the dry powder with subsequent shaking and vortexing, giving clear solutions in all cases. The concentrated stock solutions were then diluted to the required concentrations. The obtained solutions were subsequently added to glass vials in which a small amount of pyrene (thin pyrene film dried from a stock solution in ethanol) was present. The final concentration of pyrene was 5×10^{-7} M. The samples were extensively vortexed and kept in the dark for at least 12 h before the measurements.

Steady-State Fluorescence Quenching (SSFQ). The samples for SSFQ were prepared at pH 2 (10 mM HCl, 5 mM NaCl) by adding the surfactant stock solutions, prepared as described above, to vials containing a preformed thin film of pyrene. The surfactant/pyrene solutions were equilibrated (magnetic stirring) for at least 12 h in the dark. The concentration of pyrene was kept at 5×10^{-7} M. The solutions were then added to vials containing the required amount of the pyridinium surfactant quencher molecule **Q** (Figure 10; thin film dried from a stock solution of **Q** in methanol), and the samples were equilibrated with magnetic stirring for an additional 12 h (dark).

The SSFQ method is based on the procedure proposed by Turro and Yekta,[25] and the main assumptions are that (i) the quenching rate constant is much larger than the probe (pyrene) decay rate constant, meaning that no light is emitted from the probes located in micelles containing quencher and (ii) the random distribution of the probe and quencher over the micelles results in a Poisson distribution. Thus, the steady-state fluorescence at a quencher concentration [**Q**] and micelle concentration c_M is given by

$$I[\mathbf{Q}] = I_0 \exp(-[\mathbf{Q}]/c_M) \tag{5}$$

where I_0 is the fluorescence intensity in the absence of quencher. The micelle concentration is

$$c_M = ([\text{Surf}]_{tot} - \text{cmc})/N_a \tag{6}$$

where $[\text{Surf}]_{tot}$ is the total surfactant concentration and N_a is the micelle aggregation number. Thus, eq 5 can be rewritten as

$$\ln(I[\mathbf{Q}]/I_0) = -N_a\{[\mathbf{Q}]/([\text{Surf}]_{tot} - \text{cmc})\} \tag{7}$$

Pyrene was excited at 335 nm, and the emission intensity was measured at 373 (I_1) and 384 (I_3) nm.

cryo-TEM. A small drop of the sample solution was applied on a copper EM grid with a holey carbon film. The excess solution was blotted with a filter paper, leaving a thin sample film spanning the holes in the carbon film. The grid was subsequently plunged into liquid ethane for vitrification. The blotting procedure was in some cases (indicated in the figure legends) performed in a controlled environment system (25 °C) at 100% relative humidity. The vitrified specimens were transferred to a Gatan model 626 cryostage and observed in a Philips CM 120 electron microscope operating at 120 kV. The images were recorded under low-dose conditions at about −170 °C.

Theory

Theoretical Model of Vesicle ζ-Potential. The model used to calculate the vesicle ζ-potential (or surface potential) has been presented in ref 5, but a brief account will be given below. The PB cell model[26] was used to calculate the surface potential of the vesicles for a given surface charge density. To describe the general electrostatic effect, we have solved the PB equation in the

(18) Guinier, A.; Fournet, G. *Small Angle Scattering of X-rays*; Wiley: New York, 1955.
(19) Provencher, S. W. *Comput. Phys. Commun.* **1982**, *27*, 229.
(20) Henry, D. C. *Proc. R. Soc. London, Ser. A* **1931**, *133*, 106.
(21) Hunter, R. J. *Foundations of Colloid Science*; Oxford University Press: Oxford, 2001.
(22) Oshima, H.; Healy, T. W.; White, L. R. *J. Chem. Soc., Faraday Trans. 2* **1983**, *79*, 1613.
(23) O'Brien, R. W.; White, L. R. *J. Chem. Soc., Faraday Trans. 2* **1978**, *74*, 1607.
(24) Kalyanasundaram, K.; Thomas, J. K. *J. Am. Chem. Soc.* **1977**, *99*, 2039.
(25) Turro, N. J.; Yekta, A. *J. Am. Chem. Soc.* **1978**, *100*, 5951.
(26) Gunnarsson, G.; Jönsson, B.; Wennerström, H. *J. Phys. Chem.* **1980**, *84*, 3114.

spherical symmetry:[27]

$$\frac{1}{r^2}\frac{\mathrm{d}}{\mathrm{d}r}\left(r^2\frac{\mathrm{d}\phi}{\mathrm{d}r}\right) = \frac{-F}{\epsilon_0\epsilon_r}c_0[\exp(-e\phi/k_BT) - \exp(e\phi/k_BT)], \quad R < r \le b \quad (8)$$

assuming that only monovalent ions are present in the solution (15 mM buffer or 15 mM NaCl). In eq 8, ϕ is the electrostatic potential, F is the Faraday constant, r is the radial distance from the center of the vesicle, e is the elementary charge, R is the vesicle radius (80 nm), and c_0 is the salt concentration at the cell boundary [b, where $\phi(b) = 0$]. The boundary conditions specifying a solution to eq 8 are $\mathrm{d}\phi/\mathrm{d}r|_b = 0$ and $\mathrm{d}\phi/\mathrm{d}r|_R = -\sigma/\epsilon_0\epsilon_r$, where σ is the surface charge density.

In the cases of **GS1**−**GS3**, we assume that there are three equilibrium reactions at the vesicle surface that determine the vesicle surface charge density, that is, the binding of two protons and one OH^- according to

$$N(1) + H_{surf}^{+} \overset{K_1}{\rightleftharpoons} N(1)H^+ \quad (9)$$

$$N(2) + H_{surf}^{+} \overset{K_2}{\rightleftharpoons} N(2)H^+ \quad (10)$$

$$S + OH_{surf}^{-} \overset{K_{OH}}{\rightleftharpoons} SOH^- \quad (11)$$

where N(1), N(2), and S are the respective binding sites on the surfactant headgroup (or at the vesicle surface) and K_1, K_2, and K_{OH} are the equilibrium constants associated with each binding site. In the case of **GS4**, we only consider the binding of the hydroxide ions to the vesicle surface; that is, the surface charge is in this case determined by eq 11. The degree of binding (f) to the respective binding site is given by

$$f_{N(i)} = \frac{K_i[H^+]_{bulk}\exp(-e\phi_s/k_BT)}{1 + K_i[H^+]_{bulk}\exp(-e\phi_s/k_BT)}, \quad i = 1, 2 \quad (12)$$

$$f_s = \frac{K_{OH}[OH^-]_{bulk}\exp(e\phi_s/k_BT)}{1 + K_{OH}[OH^-]_{bulk}\exp(e\phi_s/k_BT)} \quad (13)$$

where ϕ_s is the surface potential. Note that only eq 13 is relevant for **GS4**. From the degree of occupancy, we calculate the surface charge density of the **GS1**−**GS3** and **GS4** vesicles according to eqs 14 and 15, respectively:

$$\sigma = \frac{e}{a_{site}}(f_{N(1)} + f_{N(2)} - f_s) \quad (14)$$

$$\sigma = \frac{-e}{a_{site}}f_s \quad (15)$$

where a_{site} is the binding-site area for the protons and hydroxide ions in the respective systems. In line with the previous publication,[5] we will assume that the binding-site areas of both the protons and the hydroxide ions are the same (110 Å^2) in the cases of **GS1**−**GS3**. However, for **GS4**, a_{site} will be treated as a fitting parameter. Using a fixed set of binding constants, we adjust the pH (assumed to be equal to $-\log[H^+]_{bulk}$) until the surface charge density in eqs 14 and 15 is the same as the surface charge density used in the solution of eq 8. The binding constants were varied until the best fit to the experimental data was obtained. The calculated potential is the surface potential (ϕ_s), which is not exactly the same as the ζ-potential because the latter is determined at some small (unknown) distance out from the vesicle surface (at the shear plane).[21] We can calculate the ζ-potential if we can estimate the location of the shear plane. It is generally recognized that the shear plane should be located a few molecular diameters out from the surface,[28,29] and considering that the surfactant sugar headgroups in the present case are rather large, we have estimated that the shear plane is located 5 Å out from the charge plane. Thus, we have calculated the ζ-potential as $\zeta \equiv \phi(R + 5\ \text{Å})$.

(27) The solution to eq 8 was obtained using the computer program PBCell. Jönsson, B. *PBCell*; Lund University: Lund, Sweden (freeware program that can be downloaded at http://www.membfound.lth.se/chemeng1/prog.html).

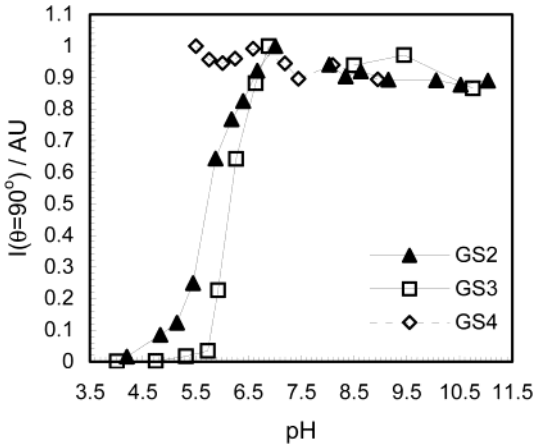

Figure 2. Scattered light intensity (normalized with respect to the highest intensity value) as a function of the pH of samples containing 0.5 mM gemini surfactant (25 °C).

Results and Discussion

Phenomenological Observations and Light Scattering. A simple but informative way of getting an overall view of the pH-dependent aggregation behavior of these systems is to measure the scattered light intensity of the dispersions as a function of the pH. The results for **GS1** have been presented in ref 5, and in Figure 2, we show similar data for **GS2**−**GS4**.

Several features may be noted. First, the scattered light intensity of the **GS2** and **GS3** dispersions decreased rapidly when the pH was lowered from around pH 7 to below pH 5. In both cases, the originally bluish/turbid dispersions became optically clear at a sufficiently low pH, indicating complete micellization. This result is in agreement with the previously published data on **GS1**, although the exact pH where the onset of the micelle formation occurs in the respective systems may differ slightly. A similar behavior has also been observed for structurally related gemini surfactants, with saturated hydrocarbon tails, in previous studies from this laboratory.[30,31] Second, around pH 7.5 (±0.3) there are no data points for **GS2** and **GS3**, which is due to a rapid vesicle flocculation in this pH region. However, the flocculated vesicles could be easily redispersed by slightly raising the solution pH, in combination with gentle magnetic stirring, resulting in dispersions with the same general appearance

(28) Frens, G.; Overbeek, J. TH. G. *J. Colloid Interface Sci.* **1972**, *38*, 376.

(29) Eisenberg, M.; Gresalfi, T.; Riccio, T.; McLaughlin, S. *Biochemistry* **1979**, *18*, 5213.

(30) Bergsma, M.; Fielden, M. L.; Engberts, J. B. F. N. *J. Colloid Interface Sci.* **2001**, *243*, 491.

(31) Fielden, M. L.; Perrin, C.; Kremer, A.; Bergsma, M.; Stuart, M. C.; Camilleri, P.; Engberts, J. B. F. N. *Eur. J. Biochem.* **2001**, *268*, 1269.

(turbid/bluish) as the original vesicle dispersions. As with **GS1**,[5] the redispersal/flocculation process was found to be completely reversible. However, the pH region of colloidal instability is slightly different for **GS1** [pH 7.1 (±0.3)] compared to that for **GS2** and **GS3** [pH 7.5 (±0.3)]. Third, the vesicle dispersions prepared from **GS4** were always turbid/bluish, and as can be seen in Figure 2, there was very little change in the appearance of the **GS4** dispersions as the pH was changed. However, for the **GS4** vesicles we also observed vesicle flocculation, but in this case, the flocculation occurred at low pH (pH ∼ 5.3). Again, the flocculated vesicles could be redispersed by titrating the sample back to a higher pH. Note that **GS4** contains oleoyl chains with 100% cis configuration, whereas **GS1**−**GS3** contain oleyl chains with 75% cis configuration (Table 1). However, we do not expect that the homogeneity of **GS4** will result in a major difference in the aggregation behavior. The characteristics of the headgroup (in particular the presence of titratable sites) will be more important in this respect.

It should also be noted that the dispersions of **GS2** and **GS3** became more viscous relative to the original vesicle dispersions at pH 5.5−4.8 and 5.8−5, respectively. This phenomenon was even more evident when the surfactant concentration was increased to 5 mM.

DLS. In previous work, we presented DLS data clearly showing the **GS1** aggregate size dependence on the solution pH.[5] In that case, the vesicles, with a diameter of ∼160 nm, were transformed into aggregates with a broad size distribution and smaller mean apparent hydrodynamic size when the pH was lowered from pH 7 to below pH 6. Further acidification of the dispersion resulted in a progressively smaller particle size until only small aggregates with a diameter on the order of 5−6 nm were obtained at pH 2. The same type of measurements have been performed for **GS2** and **GS3** with similar overall results, as is shown in Figure 3. It is noteworthy that the appearance of the aggregates with broad size distributions correlates with the intensity drop shown in Figure 2 and also the onset of a significant viscosity increase. Furthermore, the measured mean size of the redispersed **GS2** and **GS3** vesicles (pH > 8) was always very similar to the size measured below pH 7.5 (∼180 nm), indicating that the flocculation did not result in vesicle fusion (not shown). These phenomena will be discussed further when we present data from the SLS and cryo-TEM measurements (vide infra). The DLS data shown in Figure 3 clearly confirm the vesicle-to-micelle transition for **GS2** and **GS3**.

It should be noted that only marginal changes of the aggregate size took place in the studied pH interval (pH 5.3−9) for **GS4**, except at pH values below the colloidal stability limit (pH 5.3), where a rapid vesicle flocculation occurred resulting in an apparent increase of the aggregate size. The mean hydrodynamic diameter of the **GS4** vesicles was 180 (±20) nm, in accordance with the size measured for the extruded **GS1**−**GS3** vesicles.

SLS. In the pH regions (ca. pH 4.5−6) where the dispersions of **GS2** and **GS3** appeared optically clear and relatively viscous, we observed a significant angle dependence of the scattered light intensity. This result is consistent with the formation of large micelles and correlates well with previous data on **GS1**.[5] We have used eq 1 to fit the intensity data and extract the radius of gyration (R_g) of the micelles. As can be seen in Figure 4, the **GS3** data are well-described by eq 1 and equally good fits were obtained for **GS1** and **GS2** (not shown). In fact, even in the vesicular region we obtained a good fit of the data to eq 1, as is shown in Figure 4 (pH 6.64). However, in this case, there was a flattening of the curve at high

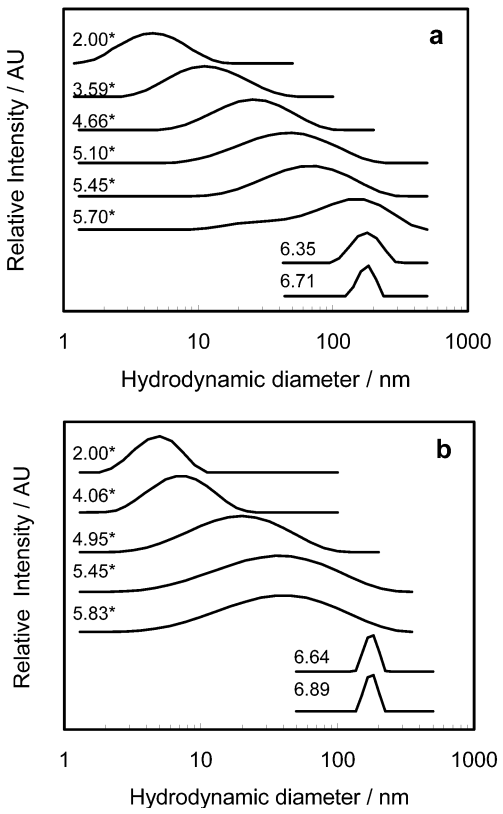

Figure 3. Size distributions obtained at $\theta = 90°$ as a function of the pH (indicated in the figure) of **GS2** (a) and **GS3** (b) samples. The surfactant concentration was either 0.5 mM or 5 mM,* and the temperature was 25 °C. The samples at pH 2 were prepared in 10 mM HCl and 5 mM NaCl, and all the other samples were prepared in a 15 mM buffer (see Experimental Section).

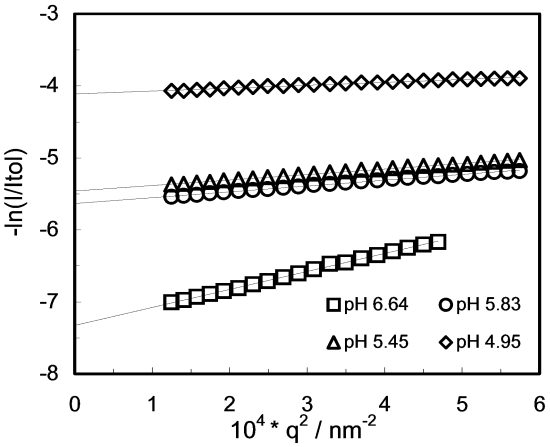

Figure 4. SLS data (normalized using toluene) from the **GS3** dispersions at 25 °C. The lines represent linear fits according to eq 1. The surfactant concentration was 5 mM in the case of the micellar samples (pH 5.83, 5.45, and 4.95) and 0.5 mM in the case of the more turbid vesicular dispersion (pH 6.64).

values of q and the fit was, therefore, performed using the data obtained in the low-q regime. Note also that there was no angular dependence of the scattered light intensity at low values of the pH, which is due to the small size of the micelles in this pH region (Figure 3).

The radius of gyration represents a different size measure compared to the hydrodynamic radius (or diameter) obtained from the DLS measurements. In particular, the ratio R_g/R_h is sensitive to the aggregate shape.[32,33] In Figure 5, we have plotted the absolute val-

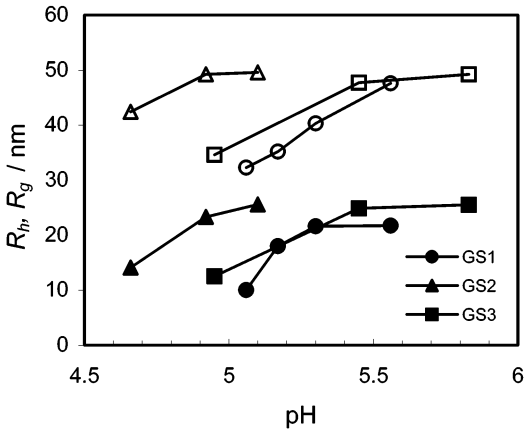

Figure 5. Hydrodynamic radius R_h (closed points) and radius of gyration R_g (open points) as a function of the pH for the dispersions containing the gemini surfactants **GS1**−**GS3**. The lines are drawn only to guide the eye.

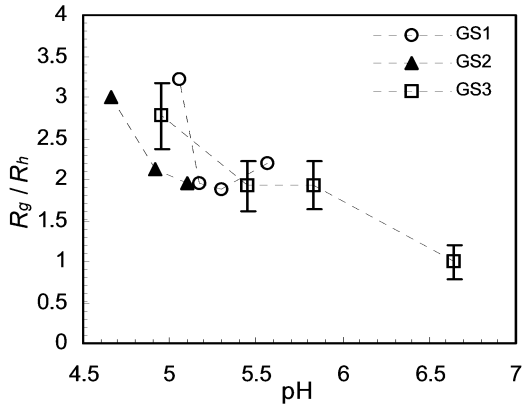

Figure 6. R_g/R_h ratio as a function of the pH. The lines going through the data points are only drawn to guide the eye. The error bars represent the estimated errors and are representative for all three systems.

ues of R_g and R_h obtained for **GS1**−**GS3** at various pH values within the micellar region.

The trends observed in Figure 5 are the same for the different systems; that is, R_g is always larger than R_h, both parameters are decreasing with decreasing pH, and the ratio R_g/R_h stays close to constant over a relatively large pH interval. The latter fact is more clearly displayed in Figure 6 where R_g/R_h is plotted as a function of the pH. An interesting feature is that the R_g/R_h ratio stays between 1.8 and 2.2 over a certain pH interval (pH 5−6) in all three systems (Figure 6). Although the exact pH interval is slightly dependent on the type of gemini surfactant, the results provide evidence that there is a common intermediate structure in the transition from vesicles to small micelles. Furthermore, the absolute magnitude, $R_g/R_h \approx 2$, is consistent with the formation of large wormlike or cylindrical micelles.[32,33] Indeed, the formation of cylindrical micelles also explains the increased viscosity in the relevant pH regions because this often is accompanied by viscosity changes in the solution. Interestingly, a pH-induced vesicle-to-cylindrical-micelle transition has been theoretically predicted for structurally related gemini surfactants using molecular dynamics and self-consistent-field calculations.[34] It may also be noted that the R_g/R_h ratio is close to 1 for the vesicular dispersion of **GS3** at pH 6.64, which is in accordance with the results obtained for spherical vesicles of low polydispersity.[35] Finally, the ratio increased to ∼3 at a lower pH in all cases, indicating a change in the aggregate structure or polydispersity.

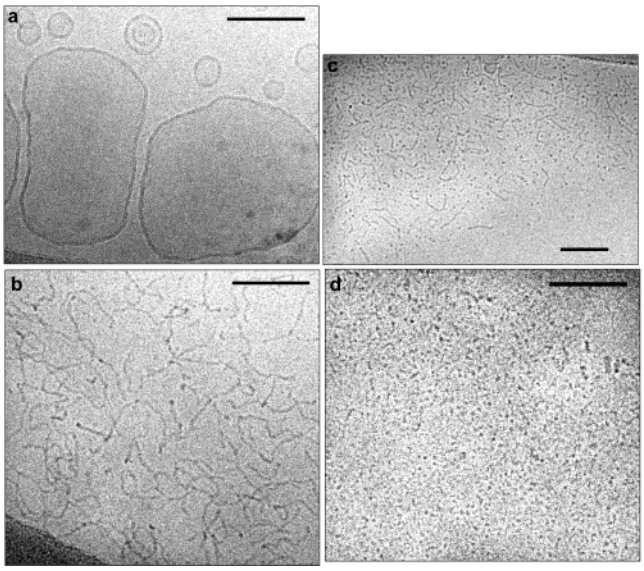

Figure 7. Cryo-TEM micrographs of **GS3** dispersions obtained at pH 7.1 (a), pH 5.4 (b), pH 4.7 (c), and pH 2.0 (d). Note wormlike micelles in part b and coexistence between wormlike and spherical micelles in part c. The spherical micelles are observed as small dark dots. The sample in part d was prepared in 10 mM HCl and 5 mM NaCl within a controlled environment system at 100% relative humidity and 25 °C. Scale bar = 100 nm.

Vesicle-to-Micelle Transition Investigated by cryo-TEM. The combined SLS and DLS experiments give a clear indication of the structural evolution of the aggregates as a function of the pH. However, the results are only indirect evidence for the proposed structural sequence. To obtain direct structural evidence, we have performed cryo-TEM measurements on the systems, and the results of these experiments for **GS3** are shown in Figure 7.

The cryo-TEM results clearly confirm the conclusions drawn from the light scattering. Furthermore, we can get some quantitative data from the micrographs. First, the bilayer thickness can be estimated to be around 4 nm (Figure 7a), which is reasonable for a bilayer consisting of a surfactant with two oleyl (C18:1) tails.[36] Second, it is clearly seen in Figure 7c that the transition from wormlike to small spherical micelles is not a gradual size decrease but that, at a certain pH, both structures coexist and there is therefore a gap in the micelle size distribution. This phenomenon has been observed before in systems with a concentration-induced micelle growth and is related to the Gibbs energy cost of creating the highly curved and slightly swollen end caps of the cylindrical micelles.[37−39] Indeed, we observed end caps that appeared to have a larger diameter than that of the cylindrical part (Figure 7b). Moreover, the onset of the formation of small micelles correlates with the increase of the R_g/R_h ratio from ∼2 to

(32) Young, C. Y.; Missel, P. J.; Mazer, N. A.; Benedek, G. B.; Carey, M. C. *J. Phys. Chem.* **1978**, *82*, 1375.
(33) Schurtenberger, P.; Cavaco, C. *Langmuir* **1994**, *10*, 100.
(34) van Eijk, M. C. P.; Bergsma, M.; Marrink, S.-J. *Eur. Phys. J. E* **2002**, *7*, 317.
(35) Penser, J.; White, G. F.; Hallett, F. R. *Biophys. J.* **2001**, *81*, 2716.
(36) Nagle, J. F.; Tristram-Nagle, S. *Biochim. Biophys. Acta* **2000**, *1469*, 159.
(37) Eriksson, J. C.; Ljunggren, S. *Langmuir* **1990**, *6*, 895.
(38) Bernheim-Groswasser, A.; Zana, R.; Talmon, Y. *J. Phys. Chem. B* **2000**, *104*, 4005.
(39) May, S.; Ben-Shaul, A. *J. Phys. Chem. B* **2001**, *105*, 630.

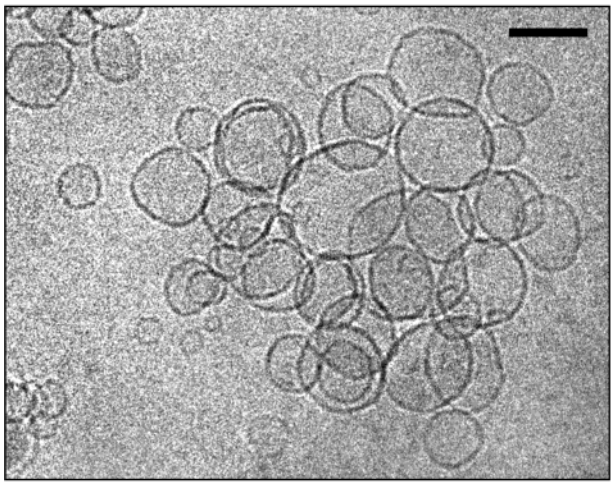

Figure 8. Cryo-TEM micrograph of the vesicles formed from **GS1** at pH 7.4. Flocculation/aggregation was induced by raising the solution pH from 6.7 to 7.4. The specimen for cryo-TEM was prepared 1 min after the pH increase, and the concentration of **GS1** was 5 mM. Scale bar = 100 nm.

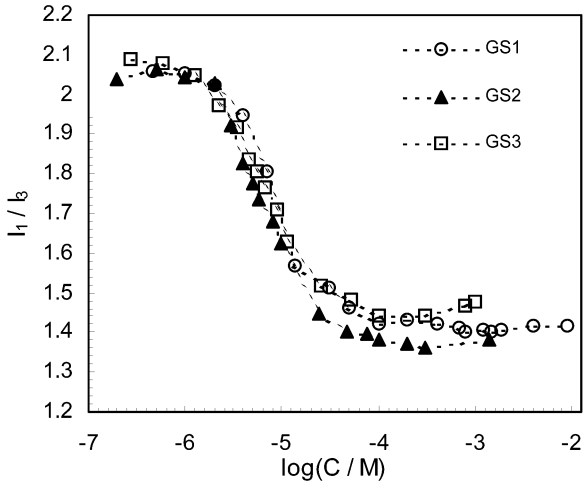

Figure 9. I_1/I_3 ratio as a function of the gemini surfactant concentration at pH 2 and 25 °C.

~3 (Figure 6), thus showing that this ratio is, indeed, a sensitive measure of the changes in the aggregate structure. Third, the small globular micelles observed at pH 2 (Figure 7d) have an estimated diameter of 4−5 nm, in good agreement with the DLS results presented in Figure 3. Finally, we expect that there should be a coexistence of cylindrical micelles and vesicles within a narrow pH region. This was confirmed for **GS1** using cryo-TEM in the pH region just above the pH (pH ~ 5.8)[5] where a complete conversion of the vesicles to cylindrical micelles occurred (not shown).

Vesicle Flocculation Investigated by cryo-TEM. The vesicle flocculation previously discussed is a reversible process, and the measured size of the aggregates after redispersal was found to be nearly identical to the size before the flocculation. Thus, the vesicles do not fuse, and the large aggregates formed must, therefore, consist of individually intact vesicles that redisperse upon appropriate changes of the solution pH. Figure 8 shows a micrograph of the vesicles formed from **GS1** that were made to flocculate by raising the pH from 6.7 to 7.4.[5] Again, the cryo-TEM result confirms the (indirect) picture obtained from light scattering, and it is clear that the floccs consist of more or less loosely aggregated vesicles. We will discuss the vesicle interactions giving rise to the flocculation in more detail when we present the data on vesicle ζ-potentials (vide infra).

cmc and Micelle Aggregation Number. The cmc values of **GS1**−**GS3** were determined using pyrene fluorescence at pH 2 (10 mM HCl, 5 mM NaCl). At this pH, we expect full protonation of the geminis and, thus, divalent cationic surfactants. The plots shown in Figure 9 were used to determine the cmc and get information about the relative polarity of the pyrene micellar binding site.

The cmc values deduced from Figure 9 are 0.0079, 0.0071, and 0.0063 mM for **GS1**, **GS2**, and **GS3**, respectively. It is clear that the nature of the sugar and spacer has little influence on the cmc. The effect of varying the spacer, from a hydrocarbon spacer to an ethylene oxide (EO) spacer, on the cmc has previously been investigated in gemini systems with similar results.[4] In fact, this result is expected because the dominating driving force for micelle formation is the hydrophobic interaction between the tails and the dominating repulsive intramicellar interaction is caused by the electrostatic interactions between the dicationic headgroups. Both the above interactions should be of similar magnitude for the **GS1**−**GS3** micelles, and, thus, nearly identical cmc values are expected. Note that we are here comparing the gemini surfactants with roughly equivalent spacer lengths and that the qualitative analysis above is not generally valid for the geminis with dissimilar spacer lengths.[4]

From the values of the I_1/I_3 ratio (1.38−1.46) at a high surfactant concentration, we conclude that the nature of the sugar and spacer has only marginal effects on the polarity of the pyrene micellar binding sites. Although the absolute magnitude of the I_1/I_3 ratio is slightly dependent on the instrumental setup, the value of around 1.4 is comparable to the values obtained for pyrene in cationic ammonium gemini systems.[40]

Before discussing the SSFQ results, a semiquantitative estimation of the micelle aggregation number N_a, based on the DLS and cryo-TEM results, will be given. The combined DLS and cryo-TEM results are consistent with those of spherical micelles with a diameter of about 4.5−5 nm at pH 2 (Figures 3 and 7d). If we assume that the hydrophilic headgroup region has a thickness of 5 Å, the resulting "hydrophobic radius" becomes 17.5−20 Å. The calculated hydrophobic volume of the micelles then becomes ~22500−33500 Å^3. The hydrophobic volume of one **GS3** surfactant molecule can be written as $2V_{C18:1} + V_{spacer} = 2(V_{CH_3} + 15V_{CH_2} + V_{CH=CH}) + 6V_{CH_2}$. Here, it is of course somewhat doubtful whether the spacer volume should actually be taken into account, and in particular, this is the case for **GS1** and **GS2** with EO spacers. Nevertheless, from the literature data[36] on the volume of the component groups, we can calculate the hydrophobic volume, $V_{hydrophobic}$, per **GS3** molecule to be ~1220 Å^3. Thus, the estimated N_a becomes 18−27. We can take this analysis one step further and estimate the area per surfactant at the hydrocarbon/water interface (a_0). On the basis of the above estimations, we get $a_0 \approx 186-214$ Å^2 at pH 2.

The micelle aggregation numbers at pH 2 were also estimated on the basis of SSFQ measurements using a pyridinium surfactant (**Q**) as the quencher (Figure 10). This type of quencher molecule has been used quite extensively[41−43] and has the obvious advantage that the

(40) Zana, R.; In, M.; Lévy, H.; Duportail, G. *Langmuir* **1997**, *13*, 5552.
(41) Hansson, P.; Jönsson, B.; Ström, C.; Söderman, O. *J. Phys. Chem. B* **2000**, *104*, 3496.

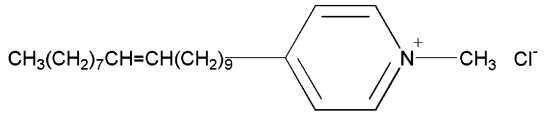

Figure 10. Structure of the pyridinium surfactant quencher molecule **Q** (double bond is cis).

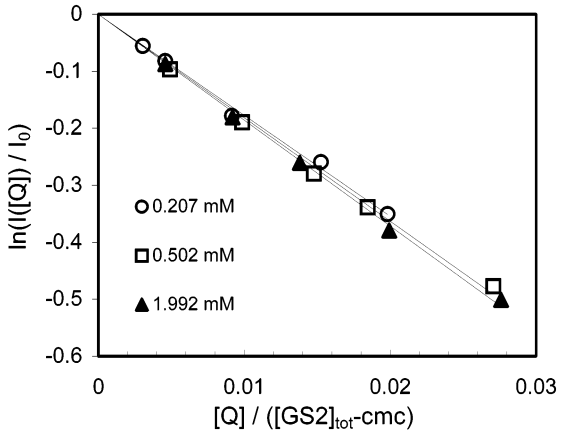

Figure 11. SSFQ data for the **GS2** samples prepared in 10 mM HCl and 5 mM NaCl (pH 2) at three different surfactant concentrations (see figure legend). The lines represent linear fits according to eq 7.

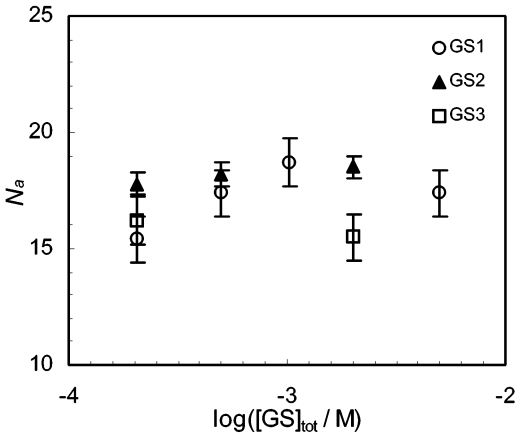

Figure 12. Aggregation number as a function of the total gemini surfactant concentration at pH 2 (10 mM HCl and 5 mM NaCl). The error bars are estimated on the basis of the measurements of the pyrene fluorescence at 373 (I_1) and 384 (I_3) nm.

quencher concentration in the aqueous pseudo subphase is minimal. This is important, especially when measuring N_a in dilute solutions. The cmc of the quencher molecule was determined in pure water using conductivity measurements and was found to be 0.20 mM. Furthermore, we have used a quencher molecule with an unsaturated hydrocarbon tail to match the tails of the gemini surfactants (Figure 10).

Figure 11 shows the data obtained for **GS2** at three different surfactant concentrations. The N_a was extracted from the linear fits of the data according to eq 7, and in Figure 12, we present the results for the three amine-containing geminis, **GS1**−**GS3**. It is clear that the aggregation number is similar for all three surfactants and that there is no significant concentration dependence in the interval investigated. The aggregation number of around 15−20 is in good agreement with the geometrical estimation given above.

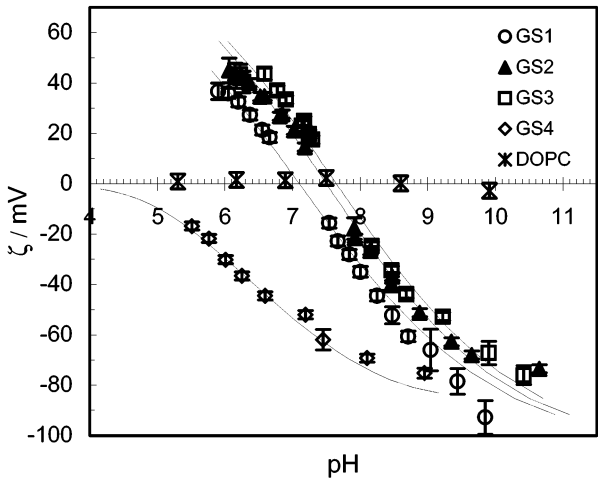

Figure 13. ζ-potential as a function of the pH for vesicles formed from **GS1**−**GS4** and DOPC in a 15 mM buffer (25 °C). The fully drawn lines represent the PB model calculations. The error bars represent standard deviation.

Vesicle ζ-Potential and Colloidal Stability. So far, we have focused on the vesicle-to-micelle transition and the properties of the micelles at acidic pH. However, equally interesting and somewhat surprising is the fact that the vesicles prepared from the compounds display a pH-dependent colloidal stability. We showed previously for **GS1** that the flocculation/redispersal process, discussed briefly above, is due to a vesicle surface charge reversal.[5] The vesicle ζ-potential is positive below a certain pH and decreases as the pH is raised. Within a certain pH interval, the net surface charge density is low and the vesicles become colloidally unstable. This is in agreement with the classical DLVO theory; that is, at low surface potentials, the attractive van der Waals interactions dominate and the vesicles aggregate/flocculate.[15] However, when the pH is gradually increased, the vesicles redisperse, and if this is related to the electrostatic part of the DLVO interaction, then it has to be due to an increased net surface charge density. Indeed, we found that the **GS1** vesicles become *negatively* charged above pH 7.1 and that the measured ζ-potential was high enough (absolute magnitude) to explain the redispersal in terms of the electrostatic interactions. We also found that the pH profile of the obtained ζ-potential could be reasonably well-described by a simple PB model in which the binding of protons and hydroxide ions to the vesicle surface is described by a number of surface equilibrium reactions. The question that arises is whether the surprisingly high affinity of the OH^- ions for the **GS1** vesicles is specific to this gemini surfactant or if the same/similar results are obtained using geminis with different characteristics such as spacer and sugar headgroup identity.

Figure 13 shows the ζ-potential profiles of all the gemini compounds (for the vesicular pH regions) together with the theoretical results obtained using the PB model. The results in ref 5 for **GS1** were calculated using the Henry equation (eq 4). However, in Figure 13, we have recalculated the ζ-potential, from the same experimental electrophoretic mobility data, using the Oshima−Healy−White theory.[22] It is clear that, independent of the type of gemini surfactant (**GS1**−**GS4**), there is binding of OH^- ions to the vesicles, giving rise to a charge reversal in the case of **GS1**−**GS3** and to negatively charged vesicles in the case of **GS4**. The latter case is especially astonishing because one, a priori, would expect the vesicles prepared

(42) Almgren, M.; Hansson, P.; Wang, K. *Langmuir* **1996**, *12*, 3855.
(43) Alargova, R. G.; Kochijashky, I. I.; Sierra, M. L.; Zana, R. *Langmuir* **1998**, *14*, 5412.

from **GS4** to be zero-charged at any pH within the investigated pH region. However, the results are in line with what has been observed for "neutral" glycolipid vesicles[9,10] and other "neutral" hydrophobic surfaces in contact with water.[11−14] It may also be noted that the colloidal stability of the **GS4** vesicles is completely determined by electrostatics because flocculation occurred below pH ∼5.3, or, in other words, when the ζ-potential became less than about −15 mV. Again, this behavior is well-predicted by the DLVO theory if we assume a nonretarded Hamaker constant, H, that is on the same order of magnitude as that found for galactolipids ($H \approx 7 \times 10^{-21}$ J).[44]

It should be emphasized that the results shown in Figure 13 are not due to the adsorption of any of the buffer substances used because we obtained essentially identical results in 15 mM NaCl (not shown). This fact also supports the use of an effective ionic strength of 15 mM 1:1 electrolyte in the calculations, also under the conditions where a 15 mM buffer was used.

Before discussing the model results, we will comment briefly on the fact that the stability of these gemini vesicles follows the expectations of the DLVO theory. In general, vesicles prepared from zwitterionic lipids, such as phosphatidyl choline (PC), are colloidally stable despite the overall zero charge (see the results for the DOPC vesicles in Figure 13). This phenomenon is generally explained by adding a number of non-DLVO interactions, such as undulation and hydration repulsion, to the total interaction potential.[45,46] If we were to follow a similar argument in the present case, then all the repulsive interactions of the short-ranged type have to be very weak for the attractive interactions to dominate, resulting in the rapid flocculation. Alternatively, the effective attractive interaction at short range is much larger in the present case compared to that of the ordinary PC vesicles. If the latter explanation is correct, then what is the mechanism? We have no answer to this question at present; however, we may allow ourselves to speculate. One possibility is that there is an enhanced effective attraction between the vesicles due to intervesicular hydrogen bonding.[47] This type of interaction would resemble the so-called bridging attraction that is known to occur in some colloid/polymer systems.[48] In the present case, this interaction must necessarily be of very short range, and close contact between the vesicles is required for it to be significant.

The previous discussion is based on the assumption that the DLVO theory is correct (at least on a semiquantitative level) and that the additional non-DLVO interactions are additive. These assumptions have been heavily criticized,[49] and the matter is further complicated by the fact that even dissolved gas can influence the stability of colloidal particles.[49] We conclude that the full picture is elusive, but the results stimulate further work.

As can be seen in Figure 13, the PB model captures the essential features of the systems. We emphasize that the derived binding constants should be regarded as estimated values and that they are derived under the assumptions that are inherent to the PB treatment of the electrostatics.[15] Furthermore, the position of the shear plane is unknown and only estimated, which puts further constraints on the accuracy of the absolute magnitude of the binding constants. Nevertheless, bearing all of the above in mind, the overall agreement between the model and the experimental results is satisfactory, providing evidence that OH^- binding is, indeed, the cause for the surface charge reversal (**GS1**−**GS3**) and negative surface charge of the "neutral" **GS4** vesicles.

Table 2. Parameters Obtained from the PB Model Calculations

compound	zpH[a]	log K_1	log K_2	log K_{OH}	a_{site}/Å^2	$\Delta G_{OH}^0/RT$[b]
GS1	7.10	8.1	6.0	8.65	110	−19.9
GS2	7.50	8.3	5.8	7.38	110	−17.0
GS3	7.65	8.5	6.0	7.30	110	−16.8
GS4	∼4.0			7.85	200	−18.1

[a] Denotes the pH where the vesicles are net 0 charged. [b] Calculated Gibbs energy for OH^- binding.

The binding constants are given in Table 2 together with the binding site areas, estimated values of the pH at which the surface charge is net 0 (isoelectric point, zpH), and derived Gibbs energies for OH^- binding, ΔG_{OH}^0.

It is clear that the main reason for the difference in the zpH between the **GS1** vesicles and the **GS2**/**GS3** vesicles is the higher affinity of OH^- for the **GS1** vesicles. The reason behind this "sugar specificity" is unclear, but it is important to realize that although the respective values of K_{OH} differ by 1 order of magnitude, the difference in the Gibbs energies is only about 2−3RT (Table 2). The relatively weak sugar specificity must, of course, be related to the mechanism of OH^- binding. In a previous paper,[5] we speculated on this mechanism based on the recent results obtained for OH^- binding to a variety of "neutral" surfaces in water.[9−14,50] One possible mechanism that has been proposed is based on the concept of a hydrophobic-surface-induced change of the water structure in the particle hydration shell.[11] This particular type of water structure, if it exists, could potentially offer favorable binding sites for OH^-. In this respect, it is interesting to note that the obtained Gibbs binding energies are on the same order of magnitude as those previously observed for binding of OH^- to glycolipid vesicles[9] and emulsion droplets.[11] Unfortunately, however, the results in the present study are not conclusive and we cannot discriminate between, for example, a mechanism that is related to the hydrophobicity of the vesicle surface and a specific interaction between OH^- and the sugar hydroxyl groups. Nevertheless, we can clearly state that the binding is not particularly sensitive to the nature of the (reduced) sugar group and the spacer identity has only a marginal effect. A feature that may be of importance is the spacer length, and this is a topic that we will examine in future studies.

The change from amines to amides in the gemini headgroups did not result in a significant change of the OH^- binding affinity (Table 2). However, to fit the ζ-potential data from the **GS4** vesicles, a larger OH^- binding site area (200 Å^2) compared to the corresponding area for the **GS1**−**GS3** vesicles (110 Å^2) was necessary (Table 2). Whether this reflects a true difference is an open question. The reason is that the calculated values of the maximum ζ-potential of the **GS4** vesicles at full OH^- binding (high pH) are −85.4 and −97.4 mV for one OH^- per 200 and 110 Å^2, respectively. Although this difference is outside the experimental error, it is too small, considering all the assumptions in the model calculations, to draw any far-reaching conclusions. To this discussion should be added that the results shown in Figure 13 for the **GS4** vesicles appear to rule out the possibility of the

(44) Marra, J. *J. Colloid Interface Sci.* **1986**, *109*, 11.
(45) Israelachvili, J. N.; Wennerström, H. *J. Phys. Chem.* **1992**, *96*, 520.
(46) Israelachvili, J.; Wennerström, H. *Nature* **1996**, *379*, 219.
(47) Schneider, J.; Berndt, P.; Haverstick, K.; Kumar, S.; Chiruvolu, S.; Tirrell, M. *Langmuir* **2002**, *18*, 3923.
(48) Israelachvili, J. *Intermolecular and Surface Forces*; Academic Press Inc.: San Diego, 1992.
(49) Alfridsson, M.; Ninham, B.; Wall, S. *Langmuir* **2000**, *16*, 10087.
(50) Pashley, R. M. *J. Phys. Chem. B* **2003**, *107*, 1714.

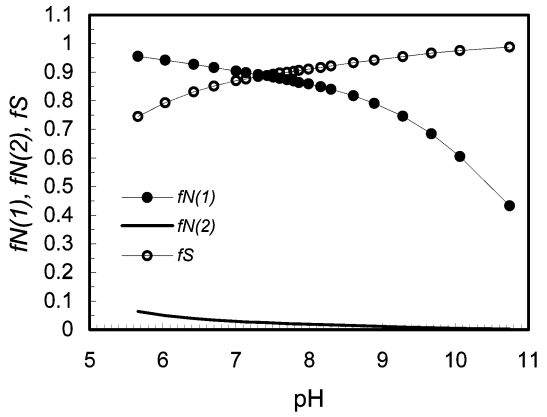

Figure 14. Fractions of protonated N(1) (*f*N(1), ●), protonated N(2) (*f*N(2), —) and occupied OH^- binding sites S (*f*S, ○) for the **GS3** vesicles as a function of the pH. The data are based on the PB model calculations (see text).

dissociation of a proton from one of the OH groups in the sugar moiety of **GS1**−**GS3**. Under the conditions of (partial) protonation of one of the nitrogen atoms in the headgroup, the OH groups might be more acidic than usual for these functionalities. However, this activation is obviously not possible in the case of **GS4**, and yet we obtain a K_{OH} that is similar to that of **GS1**−**GS3** (Table 2).

Finally, it should be noted that the binding constants given for **GS1** in Table 2 are slightly different from those given in ref 5. The reason is that we in this study have estimated the location of the shear plane and, thus, optimized the binding constants with the assumption that $\zeta \equiv \phi(R + 5\ \text{Å})$. In addition, we have here calculated the ζ-potential using the more exact theory of Oshima et al.[22] However, the overall conclusions in ref 5 remain unchanged because the difference between the derived binding constants is only marginal.

Vesicle Surface Charge and Surfactant Packing Parameter. Using the PB model, we can calculate the fraction of occupied binding sites as a function of the pH. A result from such a calculation is plotted in Figure 14 for the **GS3** vesicles.

The results in Figure 14 are quite revealing and show why the vesicles become negatively charged above the zpH (pH 7.65) because the fraction of bound OH^- is larger than the sum of the protonated N(1) and N(2) in this pH region. Furthermore, the fraction of dicationic (doubly protonated) **GS3** is relatively low, <10%, around the pH (pH 5.5−6, Figure 3b) where we observed the onset of the cylindrical micelle formation. Similar model results are obtained for **GS1**[5] and **GS2**.

To explore whether the onset of micelle formation can be explained in terms of protonation and if the conventional theories on surfactant aggregation are sufficient, we have estimated the so-called surfactant packing parameter, *P*. This parameter was introduced by Israelachvili et al.[51] and serves as a tool for predicting the surfactant aggregate morphology and phase behavior. The packing parameter is defined as follows:

$$P = V_{\text{hydrophobic}}/(a_0 l_c) \qquad (16)$$

where a_0 is the optimal cross-sectional headgroup area at the hydrocarbon/water interface and l_c is the critical chain length. We already know that the fully protonated gemini surfactants (pH 2) form small spherical micelles (Figure 7d) for which the packing parameter is $P \leq {}^1/_3$. We will, therefore, assume a value of $P = 0.33$ for the dication. In the vesicular region, we have estimated the headgroup area to be $a_0 = 110$ Å^2, and this value has been used in the PB model calculations. With $V_{\text{hydrophobic}} = 1220$ Å^3 and taking $l_c = 20$ Å, we get $P \approx 0.55$ for **GS3** in the vesicular region. This value is in agreement with the prediction for vesicles or flexible bilayers (${}^1/_2 < P \leq 1$).[51] The prediction of *P* for cylindrical micelles is ${}^1/_3 < P \leq {}^1/_2$, and if we assume that cylinders are formed in the present systems when $P = {}^1/_2$, we get the following expression:

$$X_{2+}0.33 + (1 - X_{2+})0.55 = 0.5 \qquad (17)$$

where X_{2+} is the mole fraction of the dication. From eq 17, we find $X_{2+} \approx 0.23$; that is, cylindrical micelles are predicted to form when 23% of the **GS3** molecules are doubly protonated. This is more than the about 10% obtained from the PB model calculations; however, it is in reasonable agreement with the experimental results, indicating that the simple geometrical packing criterion works also in the present gemini surfactant system. Clearly, the theoretical results also indicate that there should be significant protonation of N(2) as the pH is lowered toward pH 2, and this protonation should result in a change of the micelle size and shape. Indeed, this is exactly what we find experimentally (Figures 3 and 7).

Conclusions

The present study has demonstrated a number of extraordinary features of the sugar-based gemini surfactants **GS1**−**GS4**. For **GS1**−**GS3**, we find the following sequence of aggregation states as the solution pH is decreased from pH 11 to pH 2: anionic vesicles → flocculated vesicles → cationic vesicles → cylindrical micelles → spherical micelles. The vesicle charge reversal is, in all cases, caused by the adsorption or binding of OH^- to the vesicle surface, and the affinity of OH^- for the vesicle surface, quantified using a PB model, is remarkably high. The micelle formation at acidic pH is explained by the protonation of amines in the gemini headgroup, leading to an increased electrostatic repulsion between the headgroups. **GS4** forms vesicles over the entire pH range; however, also in this case the vesicle surface charge is determined by the binding of OH^-. In fact, despite being a neutral surfactant with no obvious titratable sites, the colloidal stability of the **GS4** vesicles is completely determined by electrostatic interactions. In all cases, the colloidal stability of the vesicles is well described by the DLVO theory.

We are at present continuing the search for a conclusive explanation for the remarkable OH^- binding. Furthermore, the vesicle-to-micelle transition within a narrow and physiologically relevant pH region may be utilized for the delivery of pharmaceutical agents as well as for gene delivery.[31,52]

Acknowledgment. M.J. gratefully acknowledges financial support from The Swedish Foundation for International Cooperation in Research and Higher Education (STINT).

Supporting Information Available: Synthesis of the gemini surfactants and the pyridinium surfactant. This material is available free of charge via the Internet at http://pubs.acs.org.

LA0343270

(51) Israelachvili, J. N.; Mitchell, D. J.; Ninham, B. W. *J. Chem. Soc., Faraday Trans. 2* **1976**, *72*, 1525.

(52) Bell, P. C.; Bergsma, M.; Dolbnya, I. P.; Bras, W.; Stuart, M. C. A.; Rowan, A. E.; Feiters, M. C.; Engberts, J. B. F. N. *J. Am. Chem. Soc.* **2003**, *125*, 1551.